Form Approved
OMB NO. 0704-0188

1. AGENCY USE ONLY (Leave Blank)	2. REPORT DATE	3. REPORT TYPE AND DATES COVERED
	February 4, 2008	Final Progress Report; 4/1/07-12/31/07

4. TITLE AND SUBTITLE
Improved Thin Film Piezoelectrics for Actuator Applications

5. FUNDING NUMBERS
W911NF-07-1-0104

6. AUTHOR(S)
Dr. Susan Trolier-McKinstry

7. PERFORMING ORGANIZATION NAME(S) AND ADDRESS(ES)
The Pennsylvania State University, Office of Sponsored Programs, 110 Technology Center Building, University Park, PA 16802

8. PERFORMING ORGANIZATION REPORT NUMBER

9. SPONSORING / MONITORING AGENCY NAME(S) AND ADDRESS(ES)
U. S. Army Research Office
P.O. Box 12211
Research Triangle Park, NC 27709-2211

10. SPONSORING / MONITORING AGENCY REPORT NUMBER
52752.1-EG-II

11. SUPPLEMENTARY NOTES
The views, opinions and/or findings contained in this report are those of the author(s) and should not be construed as an official Department of the Army position, policy or decision, unless so designated by other documentation.

12 a. DISTRIBUTION / AVAILABILITY STATEMENT
Approved for public release; distribution unlimited.

12 b. DISTRIBUTION CODE

13. ABSTRACT (Maximum 200 words)

Thin film piezoelectrics for microelectromechanical systems offer large motions, often with low hysteresis, high available energy densities, as well as high sensitivity sensors with wide dynamic ranges, and low power requirements. Among ferroelectric films, the majority of the MEMS sensors and actuators developed have utilized lead zirconate titanate (PZT) films as the transducer. Randomly oriented PZT films show piezoelectric e31,f coefficients of about – 6 to 7 C/m2 at the morphotropic phase boundary. It has recently been suggested that these coefficients are suppressed by Zr/Ti compositional gradients within the films. Consequently, the goal of this exploratory program was to prepare PZT films with different levels of compositional uniformity via chemical solution deposition, and quantify the resulting dielectric and piezoelectric constants of the films. Four different solution methods were examined. It was determined that published methods for reducing compositional gradients in PZT films were not straightforward to reproduce. Significantly better piezoelectric coefficients were obtained by using {001} oriented PbTiO3 buffer layers to prepare {001} oriented PZT films. The net result is that it was possible to double the e31,f coefficient to -12 C/m2. The resulting thin films will enable lower voltage MEMS actuators as well as improved sensor and energy harvesting systems.

14. SUBJECT TERMS	15. NUMBER OF PAGES
	13
	16. PRICE CODE

17. SECURITY CLASSIFICATION OR REPORT	18. SECURITY CLASSIFICATION ON THIS PAGE	19. SECURITY CLASSIFICATION OF ABSTRACT	20. LIMITATION OF ABSTRACT
UNCLASSIFIED	UNCLASSIFIED	UNCLASSIFIED	UL

NSN 7540-01-280-5500

Standard Form 298 (Rev.2-89)
Prescribed by ANSI Std. 239-18
298-102

Final Progress Report for Research Agreement No. W911NF-07-1-0104
The Pennsylvania State University / Dr. Susan Trolier-McKinstry, PI

Improved Thin Film Piezoelectrics for Actuator Applications

ABSTRACT

Thin film piezoelectrics for microelectromechanical systems offer large motions, often with low hysteresis, high available energy densities, as well as high sensitivity sensors with wide dynamic ranges, and low power requirements. Among ferroelectric films, the majority of the MEMS sensors and actuators developed have utilized lead zirconate titanate (PZT) films as the transducer. Randomly oriented PZT films show piezoelectric $e_{31,f}$ coefficients of about – 6 to 7 C/m^2 at the morphotropic phase boundary. It has recently been suggested that these coefficients are suppressed by Zr/Ti compositional gradients within the films. Consequently, the goal of this exploratory program was to prepare PZT films with different levels of compositional uniformity via chemical solution deposition, and quantify the resulting dielectric and piezoelectric constants of the films. Four different solution methods were examined. It was determined that published methods for reducing compositional gradients in PZT films were not straightforward to reproduce. Significantly better piezoelectric coefficients were obtained by using {001} oriented $PbTiO_3$ buffer layers to prepare {001} oriented PZT films. The net result is that it was possible to double the $e_{31,f}$ coefficient to -12 C/m^2. The resulting thin films will enable lower voltage MEMS actuators as well as improved sensor and energy harvesting systems.

STATEMENT OF THE PROBLEM
Introduction

The field of MEMS is a large and growing one, with numerous means reported for both sensing and actuation on-chip. Given the plethora of mechanisms by which the environment can be detected and/or useful responses made, it is worth considering the impetus for integrating piezoelectric thin films into MEMS devices (i.e. what advantages offset the need to introduce new materials into the cleanroom environment?). As usual, the answer to such a question depends significantly on the device or function in question. However, a couple of attributes come to the fore in promoting the use of piezoelectric devices in MEMS applications. These include:

1) The ability to perform large amplitude actuation with lower drive voltages and low hysteresis. The preponderance of MEMS literature utilizes electrostatic actuation of flexural structures. Electrostatics is relatively easy to implement, and offers the possibility of large amplitude actuation, though typically at the cost of large driving voltages and substantial hysteresis. Current-based actuation approaches, such as those utilized in many thermal and magnetically driven devices, typically require high power to operate, and in some cases are inherently slow (e.g. due to thermal time constants). In contrast, the piezoelectric effect can be utilized to drive large displacements in MEMS structures at modest voltages, low powers, and with low hysteresis.
2) Piezoelectric sensors do not require power themselves (although of course any associated electronics such as charge or voltage amplifiers, etc, will need to be powered). As a result, piezoelectric MEMS are interesting for low power requirement sensors. Indeed, in situations where the sensor is operated only on an intermittent basis, it is also possible to visualize using any such sensor in a mechanically noisy environment as a power source the remainder of the time. Such energy harvesting schemes have been implemented in bulk and thick film piezoelectrics [i,ii,iii,iv]. Moreover, as sensors, it is possible to design piezoelectric devices with broad dynamic range and low noise floors.
3) The fact that piezoelectricity shows good scaling with size. That is, the energy density available for actuation remains high, even as device sizes drop. Poor scaling is, of course, one of the principal reasons that electromagnetic motors are not attractive at MEMS size scales.
4) The straightforward ability to provide electrical signals to drive or sense the device. Much like the case of electrostatics, piezoelectrics need only electrical contact for sensing or actuation. From the point of view of electronic circuit design, piezoelectric elements are CMOS compatible. The resulting signals are easily processed on chip.

Thus, there are some application areas where integration of piezoelectric films into the device becomes practical. Considerable progress has been made in this area over the last 20 years, with devices such as filters, micromotors, micropumps, micro-sonar arrays, scanning force microscopy tips, accelerometers, etc. [v,vi,vii,viii,ix,x] having been demonstrated. The Trolier-McKinstry group has been working for >15 years on the deposition, characterization, and integration of piezoelectric thin films into MEMS devices (See Fig. 1).

Important Piezoelectric Coefficients for MEMS

The parameters needed to describe the piezoelectric effect are the strain tensor x_i, the stress tensor σ_i, as well as the electric field E_i and the electric displacement field D_i vectors. Piezoelectricity is the linear relation between the D-field and strain/stress:

$D_i = \sum_k d_{ik}\sigma_k$ *or* $D_i = \sum_k e_{ik}x_k$ These equations describe the direct effect. The d and e coefficients are related to each other through the stiffness tensor c_{ij}^E: $d_{ik} = e_{ip}c_{pk}^E$. The converse effect is described by the same set of piezoelectric coefficients:

$$x_i = \sum_k d_{ki}E_k \quad or \quad \sigma_i = -\sum_k e_{ki}E_k$$

In MEMS technology, most piezoelectric thin films are polycrystalline and the piezoelectric effect is averaged over all the grains. In ferroelectric films, the net piezoelectric effect is achieved by poling. It is conventional to assign the index 3 to this poling direction.

Thin film piezoelectrics are used in composite structures, where an underyling silicon, SiO_2, or Si_xN_y support structure is often utilized to create a unimorph (See Fig. 2). In most cases, the critical piezoelectric coefficient for piezoelectric MEMS structures is the $e_{31,f}$ coefficient. That is, the piezoelectric is electroded at the top and bottom surfaces, and the passive elastic layer is used to amplify the deflection via flexural motion of the structure.

The input and output parameters for actuator and sensor applications of piezoelectric laminated plates is schematically described in Fig. 2. In an actuator, application of a voltage leads to a piezoelectric in-plane stress causing a deflection of the structure, whereas the piezoelectric thin film is strained in the out-of-plane direction. In the sensor mode, in-plane strains create the piezoelectric charges that record the deformation of the flexible structure. In addition, the film is sensitive to out-of-plane stress (which also causes in-plane strain!). A cantilever structure can be modelled by analytical methods [xi,xii].) In the actuator mode, a constant curvature is established at a given voltage. The deflection at the end of the beam is proportional to the square of the beam length. Excursions of 10 to 20 μm with 500 μm long beams have been obtained [xiii]. More complicated structures must be analyzed by means of finite element calculations [xiv].

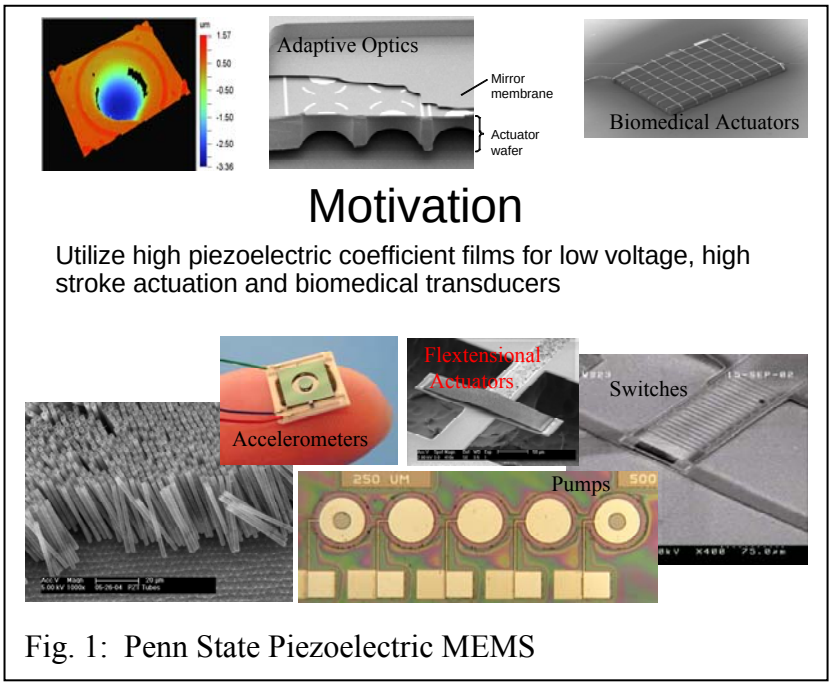

Fig. 1: Penn State Piezoelectric MEMS

There is a need to develop improved actuation approaches for MEMS in order to decrease the required drive voltages and increase the response times of devices without sacrificing the total displacement. One approach that enables this is the use of piezoelectric actuation with high piezoelectric coefficient thin films, such as $PbZr_{0.52}Ti_{0.48}O_3$ (PZT). For example, in the field of rf switches, use of PZT thin film actuators enabled actuation voltages

that average less than 10 volts, with switch operation demonstrated as low as 2 volts. The series switch exhibited excellent isolation from DC up to 65 GHz with values better than 20 dB across the frequency band and as large as 70 dB below 1 GHz (See Fig. 3).[xv] In a piezoelectrically-actuated switch for rf signals, the overall speed of the device is limited by the device size, with smaller dimensions yielding higher resonance frequencies. However, since it is imperative that a certain standoff be maintained, in order to maintain a good "on – off" ratio at high frequencies, while the device must be laterally small, it should still be possible for a vertical gap (ideally of several microns) to be maintained [[xvi]]. Further improvements in switching performance and speed could be accomplished by increasing the piezoelectric coefficients of the films.

A second example of the use of piezoelectric films in MEMS is a high frequency, high resolution ultrasound system that is currently under development at Penn State. High frequency ultrasound (50 MHz-1 GHz) is useful in imaging tissues such as the prostate, eye or skin, or organs as an endosurgical aid. Advances in ultrasound transducer technology will lead to improvements in the accuracy of diagnostics of many skin diseases including blistering diseases, diseases of skin appendages and hair diseases, benign and malignant skin tumors, investigation of wound healing, skin atrophy, and cancer. Ultrasound minimizes the need for skin biopsy, has no side effects, and provides an immediate conclusion without emotional and physical scarring. At still higher frequencies, these devices should have sub-cellular resolution, and so will be useful for tracking the behavior of *unlabeled* cells as a function of time. This, in turn, could be quite useful by allowing clinicians to study the impact of different chemotherapeutic agents with a particular cancer, potentially allowing tailored treatments to be achieved for each patient.

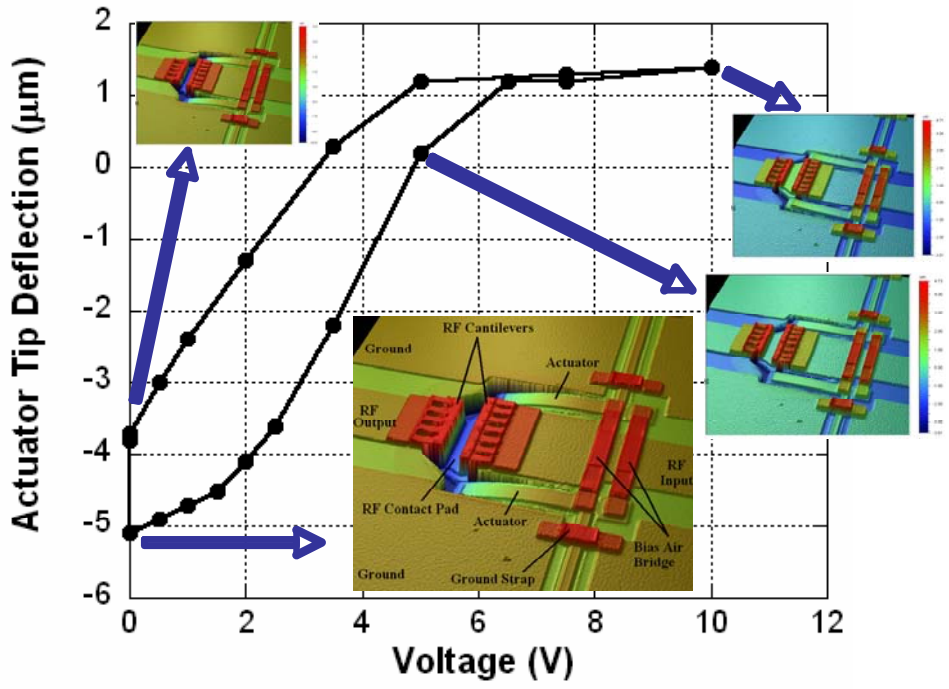

Figure 3: Army Research Laboratory/Penn State piezoelectric actuated rf switch using PZT films.

Use of thin film piezoelectrics both enables preparation of array transducers at these very high frequencies, and permits close-coupling of the electronics in a CMOS platform. The result is that the entire ultrasound system (i.e. everything but the display) can be miniaturized to about 5 mm on a side (See Fig. 4). This greatly increases the

utility of the system for catheter applications. In addition, it enables either reduced wire count, or completely wireless ultrasound systems.

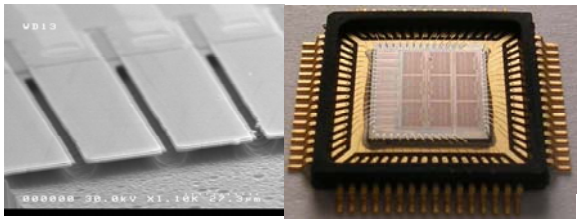

Fig. 4: First generation high frequency ultrasound transducer and CMOS drive receive circuit developed at Penn State

The $e_{31,f}$ coefficient of the PZT films used in the switches, ultrasound transducers, and the devices in Fig. 1 is about –6 to –7 C/m^2, which is typical for well-processed, randomly oriented films. However, it has recently been reported that it is possible to significantly increase the achievable piezoelectric coefficient of thin films. Thus, this program was dedicated towards developing improved piezoelectric response in PZT thin films, and in transitioning this knowledge to the Army Research Laboratory at Adelphi, Maryland, where Ron Polcawich and Madan Dubey have been leading efforts to integrate piezoelectric thin films into MEMS devices for DOD applications.

Morphotropic Phase Boundaries

The most widely utilized ferroelectric thin films for piezoelectric applications are based on lead zirconate titanate (PZT). This system illustrates many of the important features of the other ferroelectric compositions as well. The lead zirconate titanate phase diagram is dominated by a rhombohedrally distorted ferroelectric region at low Zr contents, a tetragonal region at high Ti concentrations, separated by a morphotropic phase boundary (MPB), with a sliver of monoclinically distorted perovskite at lower temperatures near the MPB [xvii]. In bulk ceramics, maxima in the piezoelectric d and e coefficients are observed at the MPB. The same behavior is often [xviii,xix,xx,xxi,xxii], but not universally [xxiii,xxiv] reported in thin films (See Fig. 5).

It is critical to note, however, that the enhancement of the properties of PZT thin films at the MPB is less strongly peaked than is the behavior shown by bulk ceramics. It has recently been suggested that part of the reason for the modest increase is associated with compositional heterogeneity in the films. That is, while the perovskite phase is lost rapidly if the Pb:Zr+Ti ratio changes, variations in the Zr:Ti ratio spatially are less readily detected via the appearance of second phases in the X-ray diffraction pattern. Thus, this program was initially aimed at increasing the piezoelectric coefficients by improving the compositional uniformity of the films.

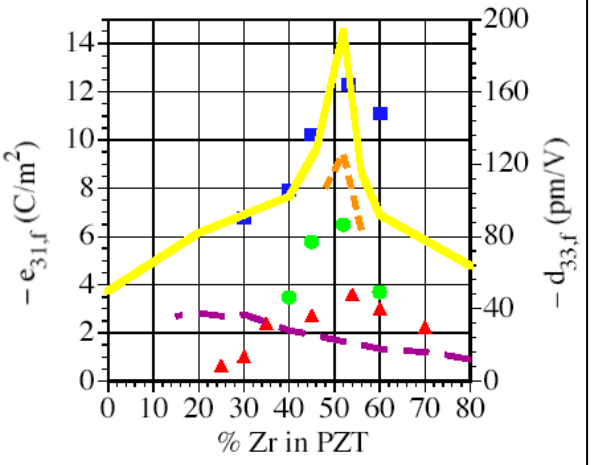

Fig. 5: Composition dependence of the relative piezoelectric response in PZT thin films. Symbols are for $e_{31,f}$ data, lines are for $d_{33,f}$ data

Summary of the Most Important Results

It was recently demonstrated by Muralt[xxv] and others that most sol-gel approaches to PZT films result in a Zr/Ti gradient for each crystallization step. The net result is that a small volume fraction of the film is actually at the morphotropic phase boundary. This substantially decreases the achievable piezoelectric coefficient. By simultaneously reducing the composition gradient in the film and increasing the lateral grain size, they were able to prepare PZT films on Si with $e_{31,f}$ coefficients of -17 to -18 C/m^2. The approach they took to minimizing the concentration gradient was to prepare four different PZT solutions with different Zr/Ti compositions, and depositing them in a reverse order of the existing composition gradient. This approach, albeit effective, is onerous. Consequently, work focused on an alternative approach.

A recent paper by Etin et al. suggests that one means of decreasing the concentration gradient in PZT films is to switch to an alternative Zr precursor, zirconium acetyl acetonate.[xxvi] At Penn State, we prepared PZT films with averaged compositions at the morphotropic phase boundary Zr:Ti = 52:48). The substrates used were commercially manufactured 375 μm Si/1 μm SiO_2/200 Å Ti/1500 Å Pt (Nova Electronic Materials, Inc.). These Pt film are primarily (111)-oriented. It was found that using the solution and film preparation conditions described in the Etin paper, there was no significant improvement in the Zr:Ti composition gradients relative to films prepared using Zr n-propoxide, as shown in Fig. 6. The net result was that there was no significant improvement in any of the functional properties. Similarly, no significant property improvement has been obtained to date either using an inverted mixing order process for the PZT or through use of commercial solution sources (Mitsubishi Materials).

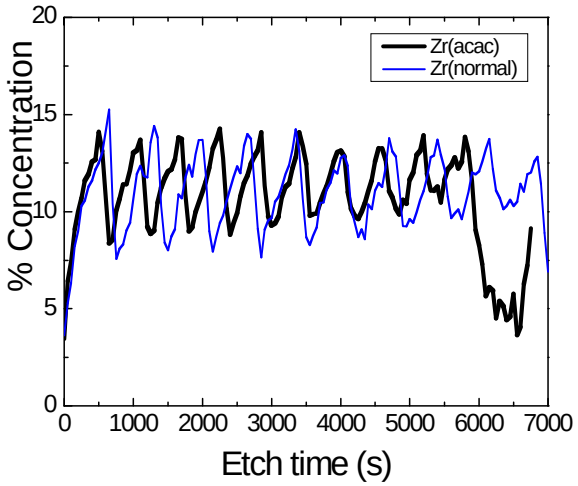

Fig. 6: Zr content as a function of depth of Chemical Solution Deposited (CSD) PZT films as measured by X-ray photoelectron spectroscopy. Each sawtooth corresponds to one crystallization step. A comparison is shown for films prepared using Zr n-propoxide (normal) and Zr acetylacetonate (acac) precursors. No significant reduction in composition gradient was found.

Significantly better results were obtained using {001} oriented PZT films. In order to prepare well oriented films, the effect of the amount of lead excess, pyrolysis temperature, and crystallization temperature of the $PbTiO_3$ buffer layer, and heating rate used during the PZT crystallization on the orientation achieved were studied. The characterization of the films is discussed in termed of morphology, dielectric, and piezoelectric properties ($e_{31,f}$).

$PbTiO_3$ buffer layer study

The $PbTiO_3$ buffer layers were chosen due to good lattice matching with PZT film, and the strong propensity for development of (001) orientation.[xxvii] Ledermann et al.[4] used 10 nm thick sputter deposited {100} oriented $PbTiO_3$ seed layers. Calame and Muralt [xxviii] achieved {100} oriented PZT films using a 20 nm thick {100} oriented $PbTiO_3$ seed layer deposited by a sol-gel technique. Kushida

et al.[xxix] demonstrated that the aging of the solution promotes (100) orientation of $PbTiO_3$ films on Pt/Si substrate due to the change of molecular size in solution and polymerization. They also studied the effect of substrate on the film orientation.

In an attempt to achieve high levels of orientation, a study of the orientation of $PbTiO_3$ layers, with two different pyrolysis temperatures and three crystallization steps was undertaken. First the $PbTiO_3$ films were pyrolyzed at 250°C for 1 min and pyrolyzed at 350°C or 400°C for 1 min. Thereafter, the $PbTiO_3$ films were crystallized at 535°C, 550°C, or 580°C for 1 min by RTA. Figure 7 shows the XRD patterns of the resulting PZT films.

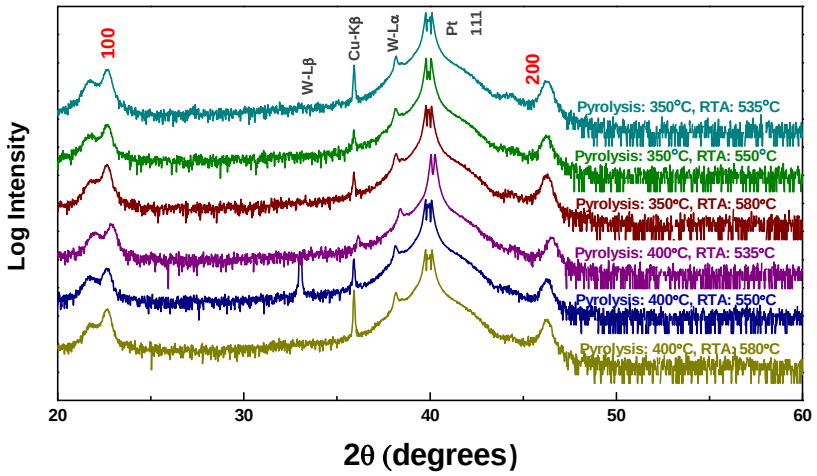

Figure 7: XRD of 30%$PbTiO_3$ buffer layers for difference pyrolysis and crystallization conditions

There is no significant difference in orientation for different pyrolysis and crystallization temperatures; in all cases, high levels of {001} orientation were achieved. Therefore, this {001} $PbTiO_3$ is suitable to use as a template layer for {001} textured PZT films. A second pyrolysis temperature of 400°C for 1 min and crystallization temperature at 580°C was chosen for subsequent buffer layer deposition.

PZT films on $PbTiO_3$ buffer layer

After deposition of one layer of $PbTiO_3$, PZT solution was spun onto the wafer at 1500 rpm for 30 sec, pyrolysed at 250°C and 400°C for 1 min and crystallized at 700°C for 1 min by RTA (which is the standard PZT film process). The steps were repeated until the desired thickness was achieved. Figure 8 shows XRD patterns of PZT films prepared in this manner with and without $PbTiO_3$ layer. It is clear that the level of {001} orientation increases when the orienting layer is used, however, a large (111) peak is still apparent. Therefore, the pyrolysis condition was modified.

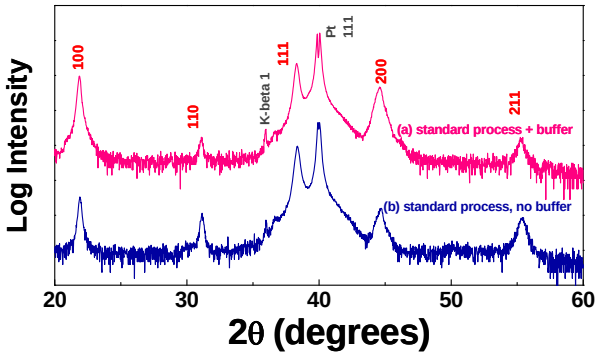

Figure 8: XRD pattern of PZT film (a) standard process on $PbTiO_3$ buffer layer (b) standard process without $PbTiO_3$ buffer layer

After $PbTiO_3$ buffer layer deposition, the 10% Pb excess PZT solution was spun onto the wafer at 1500 rpm for 30 sec, pyrolyzed at 350°C for 20 sec. The spinning and pyrolysis steps were repeated 4 times before crystallization. PZT films are crystallized at 650°C for 1 min by RTA. The heating rates were varied from 10°C/sec to 65°C/sec.

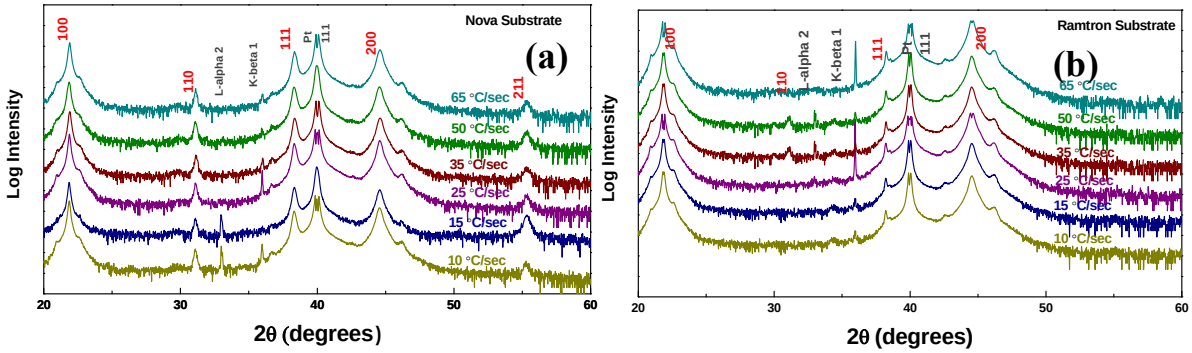

Figure 9: XRD of PZT films with $PbTiO_3$ layer onto (a) Nova substrates (b) Ramtron substrates crystallized with different heating rates

Figure 9 illustrates the XRD patterns of PZT films on $PbTiO_3$ layers as a function of the heating rate used during crystallization. The results show that there is a little effect of heating rate on orientation. In comparing the results shown in Figure 7 and Figure 8, it is obvious that both the orienting layer and the pyrolysis conditions influence the degree of {100} orientation of PZT films, while the heating rate during the RTA step does not. These data contrast with previous reports that PZT films crystallized with high heating rates develop more (111) orientation than those prepared using a low heating rate.[xxvii] The buffer $PbTiO_3$ layer used between the substrate and PZT films, should decrease heterogeneous nucleation of (111) oriented grains from the substrate.[xxx] However, some (111) orientation is still present in the films, as is a small volume fraction of pyrochlore. Future work will concentrate on preparing better-oriented films with a minimum of second phase content.

Figure 10 shows the cross sections of 0.94 μm thick PZT films on Nova and Ramtron substrates, respectively. There is some columnar microstructure to the grains. The films are dense and crack-free.

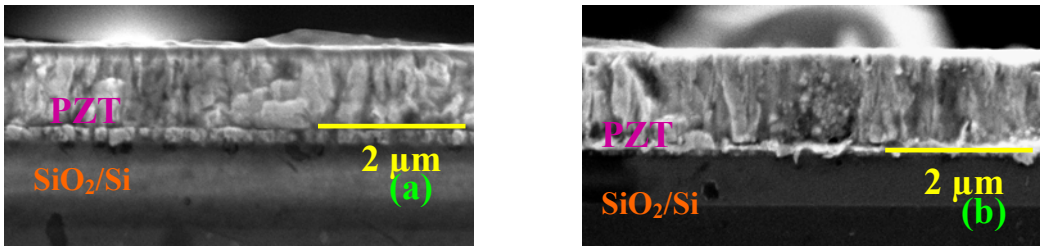

Figure 10: **Cross section of PZT film onto (a) Nova substrate (b) Ramtron substrate**

Electrical properties and piezoelectric coefficient

The electrical properties of the partially {001} oriented PZT films on Ramtron and Nova substrates were characterized. For the Ramtron substrate, the dielectric constant is 1140 with tan δ = 3.3 %, at 1 kHz. For the Nova substrate, the dielectric constant is 1060 with tan δ = 2.3 %, at 1 kHz. Comparing to Ledermann et al., the dielectric constants of both films in this work are higher than those of the reported PZT {100} 53/47, and the losses are lower.[xxxi]

Figure 11 illustrates the hysteresis loops of partially {001} oriented PZT films on Ramtron and Nova substrates, respectively. The P_r and E_c of PZT films are 18 µC/cm^2, 43 kV/cm and 22µC/cm^2, 49 kV/cm, respectively. For equivalent levels of film texture, films with lower remanent polarization values have lower $e_{31, f}$.[xxxii]

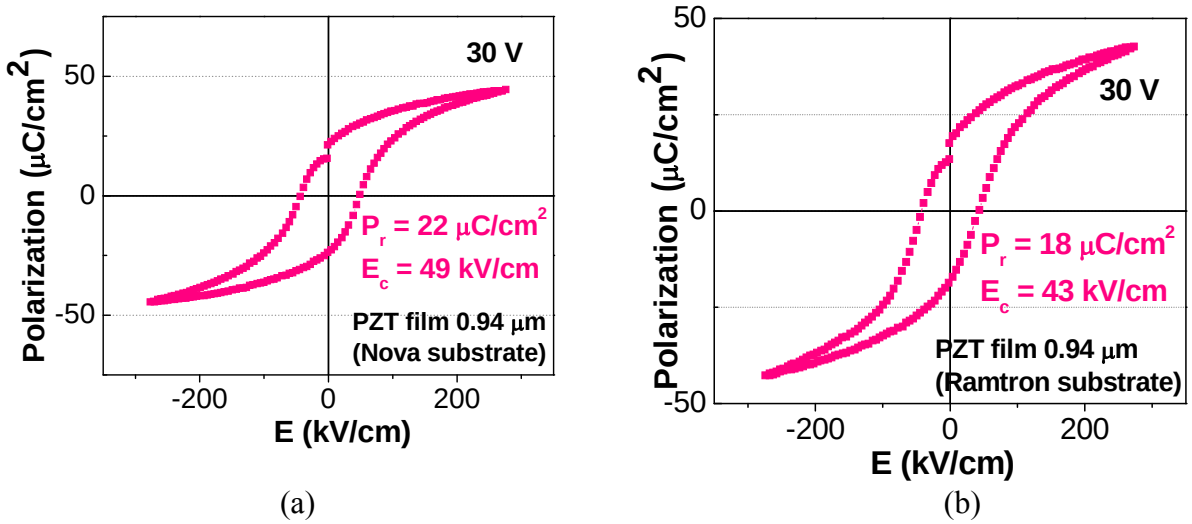

Figure 11: Hysteresis loops of PZT film on buffer layer (a) Nova substrate (b) Ramtron substrate

The concentration of Pb in the $PbTiO_3$ layer was also changed both in an attempt to reduce the amount of pyrochlore in the oriented films, and to understand the impact on the degree of {001} orientation. The high volatility of lead can create locally Pb-depleted zones, especially near the surface in Pb-based oxide thin films. The low lead content leads to formation of a parasitic pyrochlore phase that degrades the electrical and electromechanical properties.

Figure 12 shows the result of 40% Pb-excess $PbTiO_3$ layers prepared with pyrolysis temperatures of 250°C and 400°C for 1 min. There is no significant difference in orientation for different crystallization temperatures and heating rates. In all cases, high levels of {001}

orientations were achieved. Therefore, the 40% Pb excess $PbTiO_3$ templates were used for PZT film deposition.

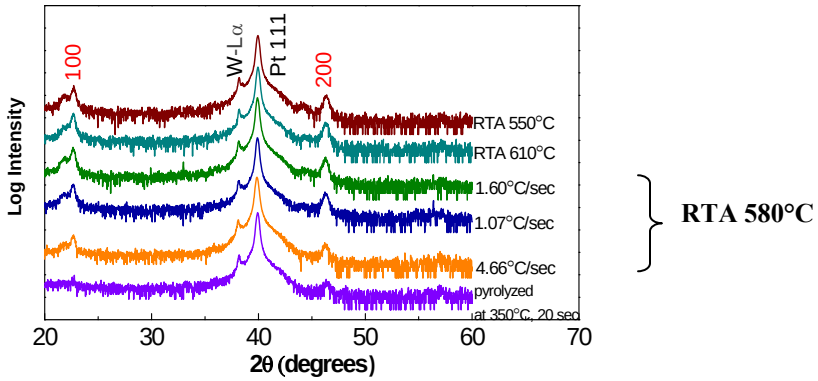

Figure 12: X-ray diffraction scans of 40% Pb excess $PbTiO_3$ layers

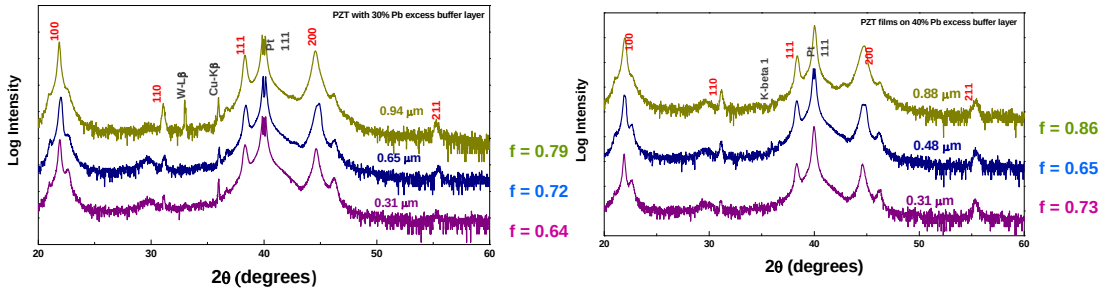

Figure 13: PZT films on (a) 30% Pb excess buffer layer (b) 40% Pb excess buffer layer

The data from Figure 13 was used to estimate the quality of the PZT film orientation. The degree of orientation was quantified using the Lotgering factor shown in Equation 1.[xxxiii]

$$f = \frac{(P - P^0)}{(1 - P^0)}$$

$$where \quad P = \frac{(I_{(100)} + I_{(200)})}{\sum I_{(hkl)}}$$

Equation 1

P was used for the texture case and P^0 for a random sample of the same composition. Higher Lotgering factors correspond to improved {100} orientation.

It can be seen that the Lotgering factor of PZT films on 40% Pb excess $PbTiO_3$ layers is higher than those on 30% Pb excess $PbTiO_3$ layers. However, all films have some amount of pyrochlore phase in XRD pattern. Therefore, additional experiments to eliminate the pyrochlore phase will be conducted in future work. Table 1 shows the electrical properties of PZT films on 30% and 40% $PbTiO_3$ buffer layers as a function of thickness. The results reveal that the permittivity of the films drops below 0.65 µm in thickness.

Table 1: Electrical properties of PZT films on 30% and 40% Pb excess buffer layers

PZT films	Permittivity (at 1 kHz)	tanδ (%) (at 1 kHz)	P_r ($\mu C/cm^2$)	E_c (kV/cm)
PZT on 30% Pb excess 0.94 µm	1060	2.3	25	40
0.65 µm	1060	4.8	17	58
0.31 µm	290	1.8	40	226
PZT on 40% Pb excess 0.88 µm	1050	4.9	18	50
0.48 µm	790	3.8	18	73
0.31 µm	330	1.4	37	279

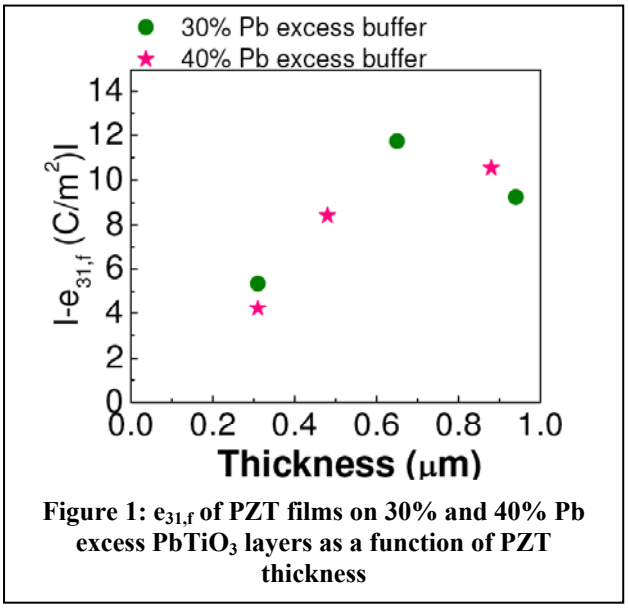

Figure 1: $e_{31,f}$ of PZT films on 30% and 40% Pb excess $PbTiO_3$ layers as a function of PZT thickness

Figure 14 shows the values of $e_{31,f}$ of PZT on 30% and 40% buffer layers as a function of thickness. For the whole range of 0.5 µm to 0.9 µm thick films, the transverse piezoelectric coefficient of -9 to -12 C/m^2 has been achieved, which is consistent with data from Ledermann et al. The $e_{31,f}$ values of the thinnest samples are about -5 C/m^2. It has to be noted that for the thinner films, the poling field was limited to 3 E_c due to a lower breakdown voltage.

The US Army Research Laboratory (ARL), Adelphi, MD has been working with Susan Trolier-McKinstry over the last 15 years in the area of piezoelectric MEMS materials, devices and characterization. The Penn State group developed a sol-gel deposition approach for lead zirconate titanate (PZT) thin films that was successfully transferred to ARL. On-going collaborations have resulted in the publication of five papers with joint PSU/ARL authorship. We are currently working (under other funding) to transfer the technology developed during this program to ARL.

Summary

Four different solution chemistries were studied to try and reduce composition gradients in PZT films. It was found that none significantly reduced the Zr/Ti gradients and increased the piezoelectric response. Thus, an alternative approach, entailing use of a $PbTiO_3$ orienting layer, provided a doubling of the achieved piezoelectric response to $e_{31,f} = -12$ C/m^2.

REFERENCES

[i] M. Umeda, K. Nakamura, and S. Ueha, "Energy storage characteristics of a piezo-generator using impact induced vibration," *Jpn. J. Appl. Phys. Part 1* **36** (5B): 3146 (1997).

[ii] G. W. Taylor, J. R. Burns, S. M. Kammann, W. B. Powers, and T. R. Welsh, "The energy harvesting eel: A small subsurface ocean/river power generator," *IEEE J. Ocean. Eng.* **26** (4), 539 (2001).

[iii] G. K. Ottman, H. F. Hofmann, G. A. Lesieutre, "Optimized piezoelectric energy harvesting circuit using step-down converter in discontinuous conduction mode," *IEEE Trans. Power Electron.* **18** (2), 696 (2003).

[iv] P. Glynne-Jones, S. P. Beeby, N.M. White, *IEE Proc. Sci. Meas. Tech.,* **148** (2) 68 (2001).

[v] J. J. Bernstein, S. L. Finberg, K. Houston, L. C. Niles, H. D. Chen, L. E. Cross, K. K. Li, and K. Udayakumar, "Micromachined High Frequency Ferroelectric Sonar Transducers," *IEEE Trans. UFFC,* **44**, 960 (1997).

[vi] Y. Nemirovsky, A. Nemirovsky, P. Muralt, and N. Setter, *Sen. and Act. A***56**, 239 (1996).

[vii] P. Muralt, M. Kohli, T. Maeder, A. Kolkin, K. Brooks, N. Setter, and R. Luthier, *Sen. and Act. A* **48**, 157 (1995).

[viii] P. Muralt, *IEEE Trans. UFFC* **47** (4) 903 (2000).

[ix] D. L. Polla and L. F. Francis, *MRS Bulletin*, **21** (7) 59 (1996).

[x] L.-P. Wang, K. Deng, L. Zou, R. Wolf, R. J. Davis, and S. Trolier-McKinstry, "Microelectromechanical Systems (MEMS) Accelerometers Using Lead Zirconate Titanate Thick Films," *IEEE Electron Device Lett.* 23, 182 (2002).

[xi] J. G. Smits and W. S. Choi, "The Constituent Equations of Piezoelectric Heterogeneous Bimorphs," *IEEE TUFFC* **38** (3), 256 (1991).

[xii] Q. Meng, M. Mehregany, K. Deng, *J. Micromech. Microeng.*, **3**, 18 (1993).

[xiii] Ph. Luginbuhl, G.-A. Racine, Ph. Lerch, B. Romanowicz, K. G. Brooks, N.F. de Rooij, Ph. Renaud, and N. Setter, *Int. Conf. Solid-State Sens. Act., Proc.,* **1**, 413 (1995).

[xiv] T. Fabula, H. Wagner, B. Schmidt, S. Buttgenbach, *Sens. Act. A* **42** (1-3), 375 (1994).

[xv] R. G. Polcawich, J. S. Pulskamp, D. Judy, P. Ranade, S. Trolier-McKinstry, and M. Dubey, "Surface Micromachined RF MEMS Ohmic Series Switch Using Thin Film Piezoelectric Actuators," submitted to IEEE – MTT (2006).

[xvi] D. Peroulis, S. P. Pacheco, K. Sarabandi, and L. P. B. Katehi, "Electromechanical considerations in developing low-voltage RF MEMS switches," *IEEE Trans. Microwav. Theory Tech.* **51** (10) 259 (2003).

[xvii] B. Noheda, D. E. Cox, G. Shirane, R. Guo, B. Jones, L. E. Cross, "Stability of the monoclinic phase in the ferroelectric perovskite $PbZr_{1-x}Ti_xO_3$," *Phys. Rev. B* **63** (1), 014103 (2001).

[xviii] H. D. Chen, K. R. Udayakumar, C. J. Gaskey, and L. E. Cross, "Electrical-Properties Maxima in Thin-Films of the Lead Zirconate Lead Titanate Solid-Solution System," *Appl. Phys. Lett.* **67** (23) 3411 (1995).

[xix] A. Seifert, N. Ledermann, S. Hiboux, J. Baborowski, P. Muralt, and N. Setter, "Processing optimization of solution derived $PbZr_{1-x}Ti_xO_3$ thin films for piezoelectric applications," *Integr. Ferro*. **35** (1-4), 1889 (2001).

[xx] F. Xu, R. A. Wolf, T. Yoshimura, and S. Trolier-McKinstry, "Piezoelectric Films for MEMS Applications," *Proc. 11th Int. Symp. Electrets*, 386 (2002).

[xxi] R. Wolf, M.S. Thesis, Penn State University (2001).

[xxii] Haccart T, Soyer C, Cattan E, Remiens D, *Ferroelectrics* **254** (1-4), 185 (2001).

[xxiii] I. Kanno, H. Kotera, K. Wasa, T. Matsunaga, T. Kamada, and R. Takayama, "Crystallographic characterization of epitaxial $Pb(Zr,Ti)O_3$ films with different Zr/Ti ratio grown by radio-frequency-magnetron sputtering" *J. Appl. Phys.* **93** (7), 4091 (2003).

[xxiv] D.-J. Kim, J.-P. Maria, A. I. Kingon, and S. K. Streiffer, "Evaluation of intrinsic and extrinsic contributions to the piezoelectric properties of $Pb(Zr_{1-X}Ti_X)O_3$ thin films as a function of composition," *J. Appl. Phys.* **93**, 5568 (2003).

[xxv] P. Muralt, IEEE Sensors Conference, Daegu, Korea (2006).

[xxvi] A. Etin, G. E. Shter, S. Baltianski, and G. S. Grader, G. M. Reisner, "Controlled Elemental Depth Profile in Sol–Gel-Derived PZT Films," J. Am. Ceram. Soc. 89 [8] 2387-2393 (2006).

[xxvii] S. Kalpat and K. Uchino, "Highly oriented lead zirconium titanate thin films: Growth, control of texture, and its effect on dielectric properties," *Journal of Applied Physics,* vol. 90, pp. 2703-2710, Sep 2001.

[xxviii] F. Calame and P. Muralt, "Growth and properties of gradient free sol-gel lead zirconate titanate thin films," *Applied Physics Letters,* vol. 90, Feb 2007.

[xxix] K. Kushida, K. R. Udayakumar, S. B. Krupanidhi, and L. E. Cross, "Origin of orientation in sol-gel-derived lead titanate films," *Journal of the American Ceramic Society,* vol. 76, pp. 1345-1348, May 1993.

[xxx] N. B. Gharb, "Dielectric and piezoelectric nonlinearities in oriented $Pb(Yb_{1/2}Nb_{1/2})O_3$-$PbTiO_3$ thin films," Ph.D. thesis in *Materials Science and Engineering*, The Pennsylvania State University, 2005.

[xxxi] N. Ledermann, P. Muralt, J. Baborowski, S. Gentil, K. Mukati, M. Cantoni, A. Seifert, and N. Setter, "{100}-textured, piezoelectric $Pb(Zr_x\ Ti_{1-x})O_3$ thin films for MEMS: integration, deposition and properties," *Sensors and Actuators A-Physical,* vol. 105, pp. 162-170, Jul 2003.

[xxxii] S. Trolier-McKinstry and P. Muralt, "Thin film piezoelectrics for MEMS," *Journal of Electroceramics,* vol. 12, pp. 7-17, 2004.

[xxxiii] K. H. Brosnan, "Processing, properties, and application of textured $0.72Pb(Mg_{1/3}Nb_{2/3})O_3$-$0.28PbTiO_3$ ceramics," in *Materials science and engineering*. Ph.D. thesis: The Pennsylvania State University, 2007.